

# Measurement of fast neutron induced $(n,\gamma)$ reaction cross-section of $^{121}\text{Sb}$ and $^{123}\text{Sb}$ in the energy range of 1 to 2 MeV

N.S.Tawade<sup>1,4\*</sup>, S.Kumar<sup>1</sup>, S.Patra<sup>1,4</sup>, R.Tripathi<sup>1,4</sup>, C.S.Datrik<sup>2</sup>, P.K.Pujari<sup>1,4</sup>  
R. G. Thomas<sup>3,4</sup>, G.Mishra<sup>3,4</sup>, A. Kumar<sup>3</sup>, S. De<sup>3,4</sup>, H. Kumawat<sup>3,4</sup>

<sup>1</sup>Radiochemistry Division, Bhabha Atomic Research Centre, Mumbai - 400085, INDIA

<sup>2</sup>Product Development Division, Bhabha Atomic Research Centre, Mumbai - 400085, INDIA

<sup>3</sup>Nuclear Physics Division, Bhabha Atomic Research Centre, Mumbai - 400085, INDIA

<sup>4</sup>Homi Bhabha National Institute, Anushaktinagar, Mumbai-400094, INDIA

\*email: [nstawade@barc.gov.in](mailto:nstawade@barc.gov.in)

## Introduction

The upcoming reactor technologies, for waste transmutation and power generation, such as Accelerator Driven Sub-critical System (ADS) and Fast Breeder Reactors (FBR) are based on fast neutron induced reactions with neutron spectrum peaking in the energy range of 1-2 MeV [1]. Measurement of fast neutron induced reaction cross-sections for long-lived and stable fission products, structural materials and heavy actinides is important for the construction and safe operation of advanced nuclear facilities. Antimony (Sb) is one of the elements widely present as a part of the structural materials in nuclear industry. The Sb metal, due to its high strength and low friction, is also used as bearing in pump for primary heat transport system [2]. So, it is important to measure the fast neutron induced reaction cross sections for Sb isotopes. The natural Sb has isotopes  $^{121}\text{Sb}$ ,  $^{123}\text{Sb}$ . In literature, there are very limited experimental  $(n,\gamma)$  reaction cross-section data available for these isotopes in 1-2 MeV neutron energy range.

In the present study, the  $(n,\gamma)$  reaction cross-section of reactor structural material  $^{121}\text{Sb}$  and  $^{123}\text{Sb}$  was measured by neutron activation technique in the neutron energy region of 1.0 to 2.0 MeV. The natural Strontium ( $^{nat}\text{Sr}$ ) was used as neutron flux monitor by considering effective reaction cross-section of combination of  $^{nat}\text{Sr}(n,\gamma)^{87}\text{Sr}^m$  and  $^{nat}\text{Sr}(n,n')^{87}\text{Sr}^m$  reactions. In order to use  $^{nat}\text{Sr}$  as flux monitor, the combined cross-section for the above reactions was measured in another study recently [3]. The experimental data from the present study have been compared with the theoretical calculations using the code TALYS 1.8 as well as the cross-section data available in the literature.

## Experimental Details

The natural oxide of antimony ( $\text{Sb}_2\text{O}_3$ ) along with natural strontium carbonate ( $^{nat}\text{SrCO}_3$ ) salt as neutron flux monitor was used in the present experiment. The monitor was mixed with sample and different circular pellets of samples were prepared. The sample was covered with  $0.075 \text{ g/cm}^2$  thick  $\text{B}_4\text{C}$  layer and  $0.4 \text{ g/cm}^2$  thick Cd foil

from both sides to avoid interference from low energy neutrons. The experiment was conducted at two different neutron energies: 1.54 and 2.0 MeV. The neutron irradiations were carried out at Folded Tandem Ion Accelerator (FOTIA), Bhabha Atomic Research Centre, Mumbai, India. The quasi-mono energetic neutron beam was generated by bombardment of energetic proton beam on  $^7\text{Li}$  ( $4 \text{ mg/cm}^2$ ) target, mounted in vacuum on inner surface of a steel flange. The sample was mounted at a distance of 1.5 mm from  $^7\text{Li}$  target, on the outer surface of the flange, in air so that the neutron beam generated in  $^7\text{Li}(p,n)^7\text{Be}$  reaction falls directly on the sample. Long irradiations (each of  $\sim 24$  hrs) were carried out at the two different neutron energies with proton current of about  $\sim 50\text{nA}$ . The temporal mapping of the neutron flux was carried out at a time interval of  $\sim 0.5$  sec during the irradiation using a scintillation detector.

## Results and Discussions

The average neutron beam energy was calculated by a Monte-Carlo code developed at BARC [4]. The radioactivity of the activation products were measured by high resolution gamma-ray spectrometry using a coaxial HPGe detector coupled to a 4K multi-channel analyzer. The net peak area under characteristic gamma-rays was used to obtain the radioactivity of the activation products at the end of irradiation, which was further used to obtain their formation cross-sections. The small variations in the neutron flux during irradiation were accounted with the help of neutron flux mapping spectrum. The total irradiation period was divided into small intervals ( $\Delta t$ ) of  $\sim 0.5$  sec. The activity produced during each small irradiation time interval was calculated with decay correction and added to obtain gross activity produced at the end of irradiation.

**Table 1:**  $(n,\gamma)$  reaction cross-section

Neutron Energy (MeV)	$^{121}\text{Sb}(n,\gamma)^{122}\text{Sb}$ Cross-section $\sigma$ (mb)	$^{123}\text{Sb}(n,\gamma)^{124}\text{Sb}$ Cross-section $\sigma$ (mb)
$1.54 \pm 0.21$	$106.4 \pm 7.7$	$70.6 \pm 9.5$
$2.00 \pm 0.23$	$71.1 \pm 2.6$	$57.9 \pm 3.8$

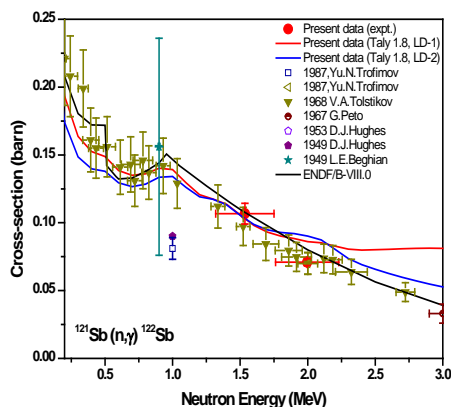


**Fig. 1** Cross-section Vs. neutron energy for  $^{121}\text{Sb}(n,\gamma)^{122}\text{Sb}$  reaction.

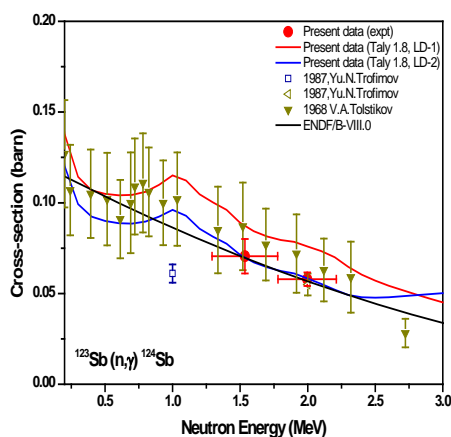


**Fig. 2** Cross-section Vs. neutron energy for  $^{123}\text{Sb}(n,\gamma)^{124}\text{Sb}$  reaction.

The full energy peak efficiency calibration of the detector was carried out using standard point sources of  $^{152}\text{Eu}^g$  and  $^{133}\text{Ba}^g$ . The characteristic gamma-ray peaks at 564.24 keV ( $^{122}\text{Sb}$ ), 602 keV ( $^{124}\text{Sb}$ ) and 388.5 keV ( $^{87}\text{Sr}^m$ ) were used to calculate the activities of the reaction products [5]. The cross-sections for  $^{121}\text{Sb}(n,\gamma)^{122}\text{Sb}$  and  $^{123}\text{Sb}(n,\gamma)^{124}\text{Sb}$  reactions are measured at two different neutron energies and summarised in Table 1. The  $(n,\gamma)$  reaction cross-sections for these reactions were also calculated using TALYS-1.8 code [6]. The measured cross-section data with TALYS calculation, existing literature and ENDF database [7] are shown in Fig. 1 and 2. The measured data could be reasonably reproduced with TALYS calculations and were also in reasonable agreement with the data of Tolstikov [8] and Trofimov [9]. As seen from the figure, there was only one data at 1.5 MeV and 2 MeV for  $^{121}\text{Sb}(n,\gamma)^{122}\text{Sb}$  reaction. Similarly, for  $^{123}\text{Sb}(n,\gamma)^{124}\text{Sb}$  reaction, there was only one data at 1.5 MeV and two data at 2 MeV. The present data

with improved uncertainty will help in better constraining of the cross-section evaluation as well as theoretical calculations. For TALYS calculations, constant temperature Fermi gas level density models (LD-01 and LD-02) were considered with a fine adjustment of level density parameter ‘ $a$ ’, pairing constant ‘ $A$ ’, parameter, average radiative width parameter ‘ $\Gamma_\gamma$ ’ and pairing energy parameter ‘ $\delta$ ’ [6].

## Conclusions

Cross-sections have been measured for  $^{121}\text{Sb}(n,\gamma)^{122}\text{Sb}$  and  $^{123}\text{Sb}(n,\gamma)^{124}\text{Sb}$  reactions at neutron energies of 1.54 and 2.0 MeV by neutron activation followed by off-line gamma-ray spectrometry using  $^{nat}\text{Sr}$  as a neutron flux monitor. The measured  $^{121}\text{Sb}(n,\gamma)^{122}\text{Sb}$  and  $^{123}\text{Sb}(n,\gamma)^{124}\text{Sb}$  reaction cross-sections obtained with improved uncertainties in the present work have been found to have reasonable agreement with literature data and ENDF prediction. It adds an independent data set using a different monitor to the cross section data base in 1-2 MeV region for the above reaction for which there are limited measurements. The experimental cross sections could be reasonably reproduced TALYS-1.8 calculations using Fermi gas level density prescription with slight adjustment in level density parameter ‘ $a$ ’, pairing constant parameter ‘ $A$ ’, average radiative width parameter ‘ $\Gamma_\gamma$ ’ and pairing energy parameter ‘ $\delta$ ’.

## Acknowledgements

Authors thank the staff members of FOTIA at Van de-Graff, BARC Mumbai for their excellent co-operation during the experiment.

## References

1. C. H. Pyeon, M. Yamanaka, Song-Hyun Kim, Thanh-Mai Vu, T. Endo, W. Fredrik, G.V. Rooijen, G. Chiba, J. Nucl. Eng. Technol. 49(6), 1234-1239 (2017).
2. S.S.Keny, A.G.Kumbhar, A Sanjukta, S.Pandey, S.Ramanathan, G.Venkateswaran, J. Curr. Sci. 106(8), 25(2014).
3. N.S.Tawade, R. Tripathi, T.N. Nag, S. Patra, C.S. Datrik, P.K. Pujari, R.G. Thomas, G. Mishra, A. Kumar, S. Dey, H. Kumawat, 15<sup>th</sup> DAE BRNS Symposium NUCAR-2021,40 (2022), Mumbai
4. H. Kumawat and V. S. Barashenkov, Euro. Phys. J. A26, 61 (2005).
5. Nuclear Data Centre Web site for Spectroscopic data : <https://www.nndc.bnl.gov/exfor/>
6. TALYS manual 1.8.
7. ENDF/B-VIII.
8. V. A. Tolstikov, V. P. Koroleva, V. E. Kolesov, A. G. Dovbenko, Yu. N. Shubin, J. Soviet Atomic Energy, 24, 709 (1968).
9. Yu. N. Trofimov, *International conference on Neutron Physics*, Kiev, 3, 331 (1987).